

1 **Polypyrrole and Activated Carbon Enriched MnCo<sub>2</sub>O<sub>4</sub> Ternary Composite as**  
2 **Efficient Electrode Material for Hybrid Supercapacitors**

3 **Simran Kour, Pawanpreet Kour, A. L. Sharma\***

4 Department of Physics, Central University of Punjab, Bathinda, Punjab, India-151401

5 \*Corresponding author: [alsharma@cup.edu.in](mailto:alsharma@cup.edu.in)

6 ***Supporting Information (SI)***

7 **1. Electrode preparation method**

8 The electrodes were prepared by blending the synthesized active material, PVDF (binder), and  
9 carbon black (conductive element) in a ratio of 8:1:1 to get consistent slurry with the addition of  
10 N-Methyl-2-pyrrolidone (NMP). Nickel foam with area of 1 cm<sup>2</sup> was then coated with this slurry  
11 and dried at 60 °C overnight. The separator (Whatman paper) wetted by 6M KOH electrolyte was  
12 sandwiched between the two electrodes (cathode and anode) and pressed using a hydraulic press  
13 to get the desired cell configuration.

14 **2. Electrochemical measurements**

15 The capacitive response of the electrode material corresponding to a voltage window of -1 to  
16 +1V was evaluated from CV and GCD in 2-electrode configuration. The EIS analysis was  
17 carried out for 10<sup>5</sup>-0.1 Hz of frequency at open-circuit voltage. For asymmetric supercapacitor,  
18 the voltage range was 0-1.6 V. The Formulae used for determining various parameters such as  
19 specific capacitance, energy density, and power density has been provided in **Table S1**.

20

**Table S1:** Formulae used for finding various parameters.

Parameter	Formula	Terms used
Bragg's law	$2d\sin\theta = n\lambda$	'd' is inter-planar spacing, '2θ' is bragg's diffraction angle, 'n' is an integer, λ is the wavelength of X-ray.
Interplanar spacing	$d = \frac{1}{\sqrt{\frac{h^2}{a^2} + \frac{k^2}{b^2} + \frac{l^2}{c^2}}}$	(hkl) are miller indices of lattice plane, (a, b, c) are lattice parameters of the crystal.
Crystallite size, D (Schherrer equation)	$D = \frac{K.\lambda}{\omega \times \cos\theta}$	K is a constant, λ is the wavelength of X-ray, 'ω' is the FWHM, '2θ' is bragg's diffraction angle.
Specific capacitance, $C_{sp}$ for single electrode (from CV)	$C_{sp} = \frac{\int IdV}{m \times v \times dV}$	'I' is the current, dV is the potential window, 'm' is the mass of active material, 'v' is the scan rate.
Specific capacitance, $C_{sp}$ for single electrode (from GCD)	$C_{sp} = \frac{2 \times I \times \Delta t}{m \times dV}$	'I' is the current, 'dt' is the discharging time, 'm' is the mass of active material.
Specific capacitance, $C_{sp}$ for SSC/ASC (from GCD)	$C_{sp} = \frac{I \times \Delta t}{m \times dV}$	'I' is the current, 'dt' is the discharging time, 'm' is the mass of active material.
Energy density, $E_d$ (from GCD)	$E_d = \frac{C_{sp} \times (dV)^2}{7.2}$	' $C_{sp}$ ' is the specific capacitance, dV is the voltage window.

Power density,  $P_d$

(from GCD)

Coulombic efficiency,  $\eta$

Response time,  $\tau$

(from EIS)

$$P_d = \frac{E_d \times 3.6}{\Delta t}$$

' $E_d$ ' is the energy density,  $\Delta t$  is the discharging time.

$$\eta = \frac{t_d \times 100}{t_c}$$

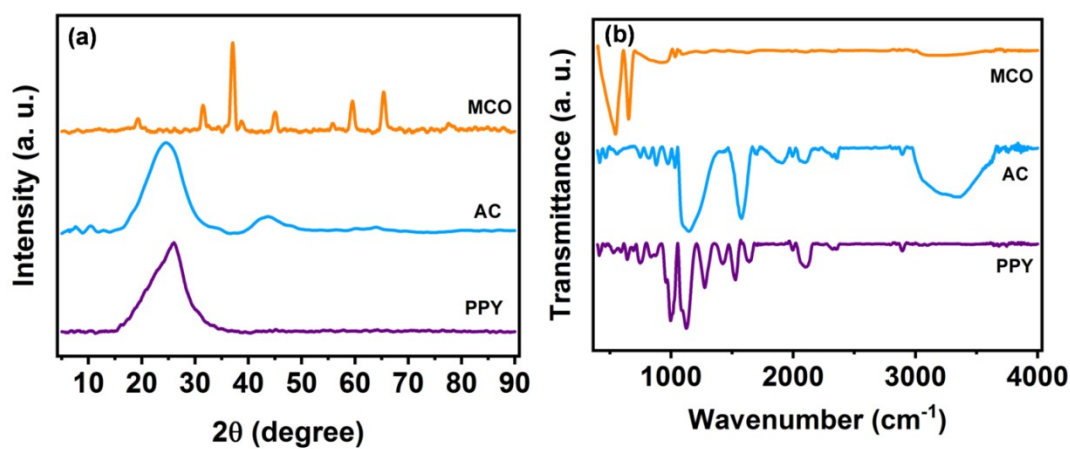
' $t_d$ ' is the discharging time and ' $t_c$ ' is the charging time.

$$\tau = \frac{1}{\nu}$$

' $\nu$ ' is the frequency corresponding to phase angle  $\theta = 45^\circ$ .

22

### 23 3. Results and Discussion



24

25

**Fig. S1:** (a) XRD and (b) FTIR patterns of MCO, AC, and PPY.

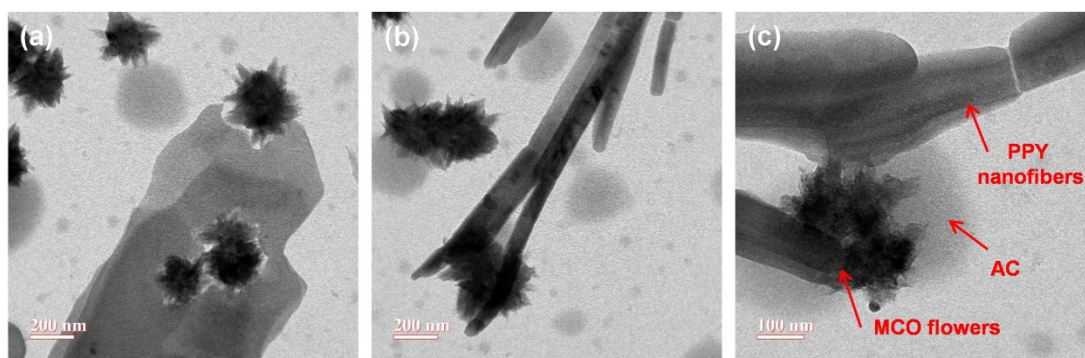
26

**Table S2:** XRD analysis for  $\text{MnCo}_2\text{O}_4$  (MCO) microspheres.

Angle	Lattice plane	Interplanar	Crystallite
$2\theta$ (degree)	(hkl)	spacing, d (Å)	size (nm)
19.3	(111)	4.6	9.1

31.5	(220)	2.8	11.2
37.1	(311)	2.4	11.1
38.7	(222)	2.3	11.9
45.3	(400)	2.0	11.4
55.5	(422)	1.6	14.2
59.5	(511)	1.5	10.7
65.3	(440)	1.4	10.6

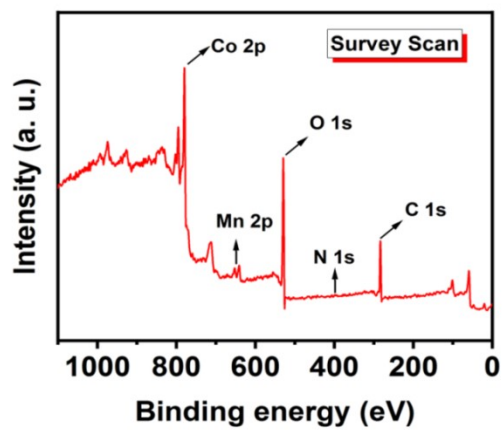
27



28

29

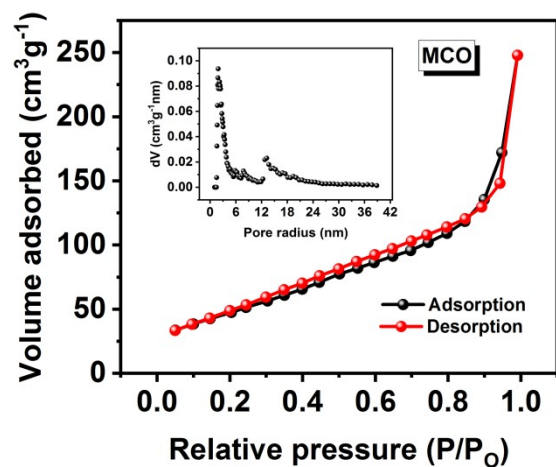
**Fig. S2: (a-c) TEM images of MAP-20 at different resolutions.**



30

31

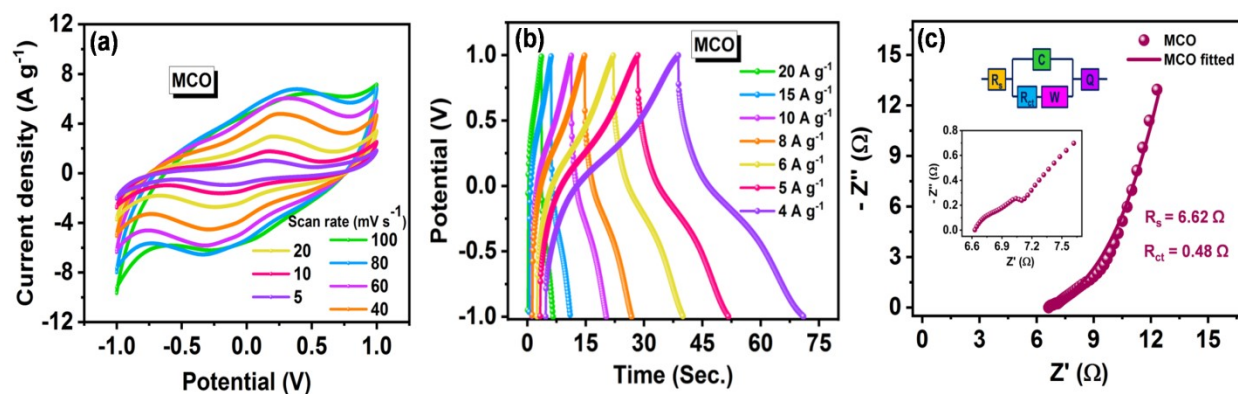
**Fig. S3: XPS survey scan of MAP-20.**



32

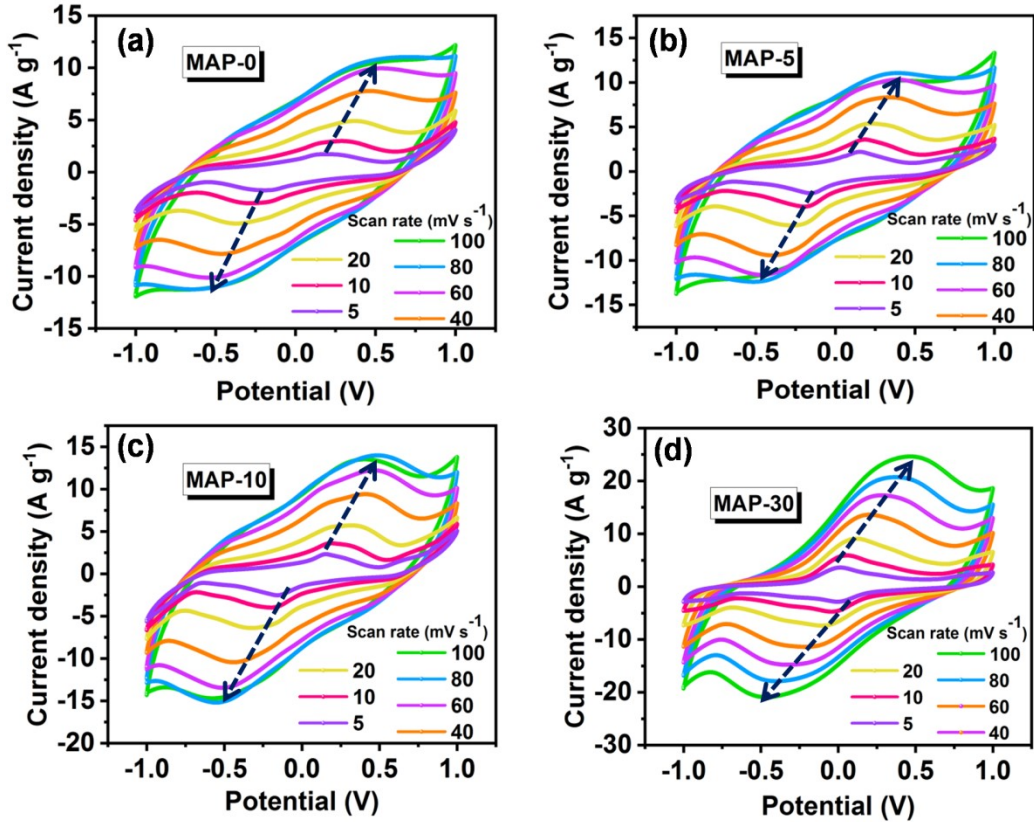
33

**Fig. S4:** BET analysis of pristine MnCo<sub>2</sub>O<sub>4</sub> (MCO).



34

**Fig. S5:** (a) CV curves of MCO, (b) GCD curves of MCO and (c) Nyquist plot of MCO with fitted circuit.



37

38

**Fig. S6: (a-d) CV of MAP-x (x = 0, 5, 10, and 30) at various scan rates.**

39 **Power law**

40 The power law gives the correlation of the current ( $i$ ) and scan rates ( $v$ ) as follows:

41 
$$i = av^b \tag{S1}$$

42 where,  $a$  and  $b$  are adjustable constants.

43 **Trasatti method**

44 The total capacitance  $C_T$  of the electrode material is given by the combination of capacitance

45 contribution of outer surface ( $C_o$ ) and inner surface ( $C_i$ ) and is given by the following formula:

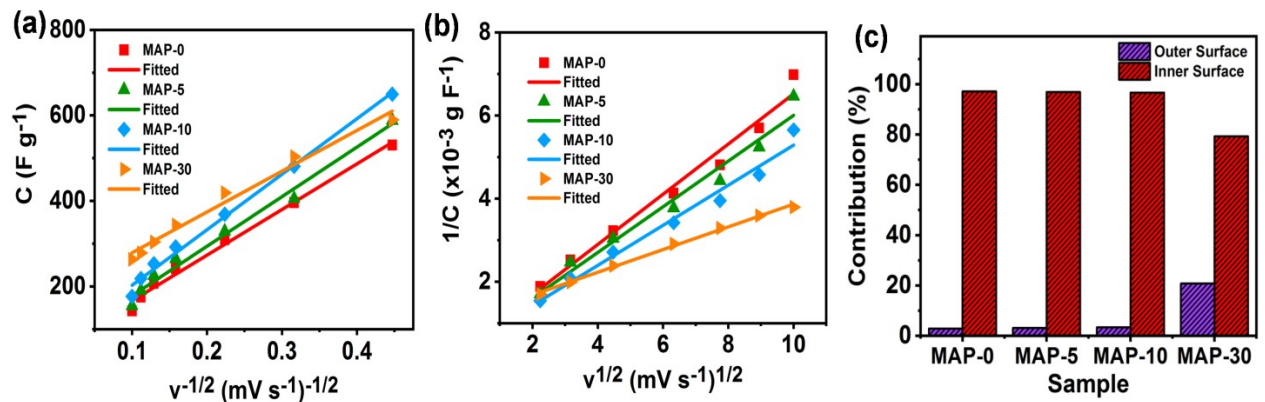
46  $C_T = C_o + C_i$  (S2)

47  $C = const. \times v^{-1/2} + C_o$  (S3)

48  $\frac{1}{C} = const. \times v^{1/2} + \frac{1}{C_T}$

49 (S4)

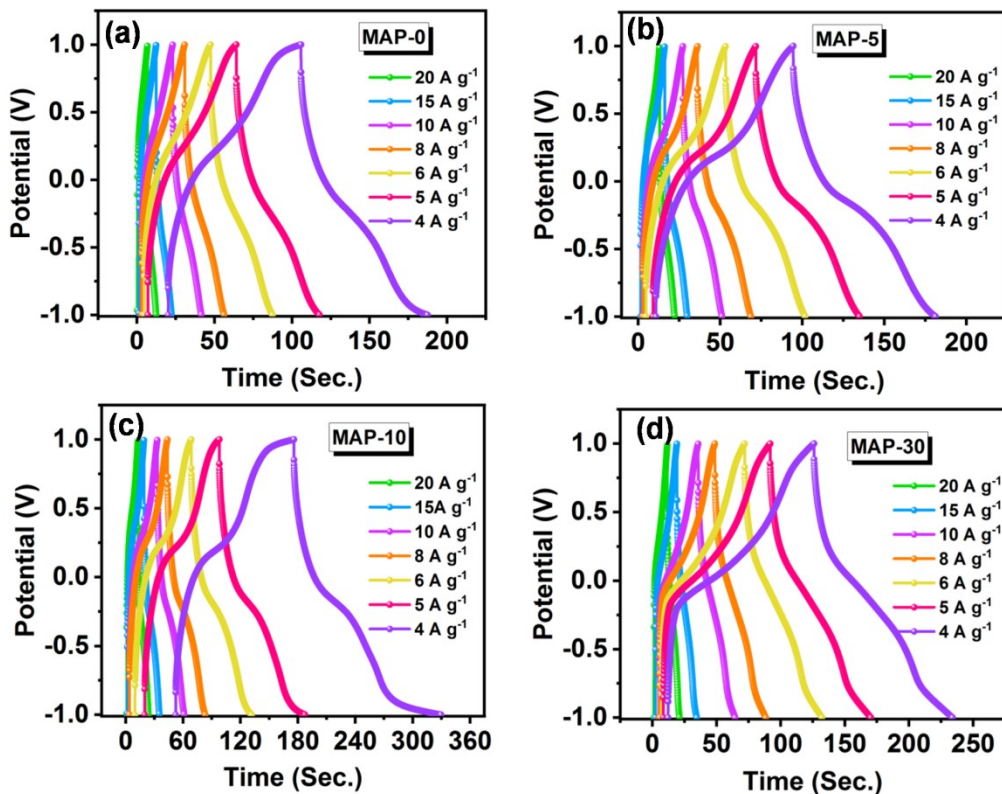
50 where,  $C$  is the sp. capacitance calculated from the CV data.



51

52

**Fig. S7: (a-c) Charge storage kinetics of MAP-x (x = 0, 5, 10, and 30).**



53

54

**Fig. S8:** (a-d) GCD of MAP-x ( $x = 0, 5, 10,$  and  $30$ ) at various scan rates.

55

**Table S3:** Comparison of supercapacitive performance of the prepared samples with literature.

Material	$C_{sp}$ ( $Fg^{-1}$ )	Voltage window (V)	ASC/SSC	$E_d$ ( $Wh kg^{-1}$ )	Pd ( $kW kg^{-1}$ )	Stability, % (cycles)	Reference
$NiCo_2O_4/NF@PPY$	1717 $C g^{-1}$	0-1.6	ASC	68.9	1.77	89.2 (10,000)	<sup>1</sup>
$MnCo_2O_4-$ graphite@PPY	2364	0-1.6	ASC	25.7	16.1	85.5 (10,000)	<sup>2</sup>
$NiCo_2O_4@PPY$	2244	0-1.6	ASC	58.8	0.36	89.2	<sup>3</sup>



---

	(1 A g <sup>-1</sup> )					(5,000)	
NiCo <sub>2</sub> O <sub>4</sub> /CNF@PPY	910	0-1.5	ASC	40.8	0.73	88.0	4
	(1 A g <sup>-1</sup> )					(10,000)	
NiCo <sub>2</sub> O <sub>4</sub> /Co <sub>3</sub> S <sub>4</sub> /MnS @PPY	2557	0-1.6	ASC	81.1	0.80	83.6	5
	(1 A g <sup>-1</sup> )					(20,000)	
MgCo <sub>2</sub> O <sub>4</sub> /PPY	988	0-1.6	ASC	40.0	1.54	84.0	6
	(1 A g <sup>-1</sup> )					(10,000)	
MnNi <sub>2</sub> O <sub>4</sub> /PPY	304	0-1.6	ASC	35.9	0.80	--	7
	(1 A g <sup>-1</sup> )						
CC@NiCo <sub>2</sub> O <sub>4</sub> @PPY	1687	0-1.5	ASC	46.5	0.72	80.0	8
	(1 A g <sup>-1</sup> )					(10,000)	
NiCo <sub>2</sub> O <sub>4</sub> @PANI	561	0-1.2	ASC	6.4	0.28	86.2	9
	(10 mV s <sup>-1</sup> )					(3,000)	
ZnCo <sub>2</sub> O <sub>4</sub> @PANI	720	0-0.5	--	--	--	96.4	10
	(10 mV s <sup>-1</sup> )					(10,000)	
CuCo <sub>2</sub> O <sub>4</sub> /GO@PANI	312.7	0-1.2	SSC	62.5	5.99	84.2	11
	(1 A g <sup>-1</sup> )					(5,000)	
CoFe <sub>2</sub> O <sub>4</sub> /PANI/GO	346.9	0-1.2	SSC	69.3	5.98	79.0	12
	(1 A g <sup>-1</sup> )					(5,000)	

---

---

Fe-MnCo <sub>2</sub> O <sub>4</sub> @PPY	422.4 (2 mA cm <sup>-2</sup> )	0-1	SSC	519.9 mWh cm <sup>-2</sup>	--	94.7 (7,000)	<sup>13</sup>
NiMoO <sub>4</sub> /rGO/PANI	1150 C g <sup>-1</sup> (1 A g <sup>-1</sup> )	0-1.7	ASC	82.43	0.85	94.5 (10,000)	<sup>14</sup>
NiCo <sub>2</sub> O <sub>4</sub> /CF@PANI	369 mAh g <sup>-1</sup>	0-1.5	ASC	60.6	2.32	--	<sup>15</sup>
MnCo <sub>2</sub> O <sub>4</sub> -AC@PPY	945.77 (5 mV s <sup>-1</sup> )	0-1.6	ASC	88.12	1.6	89.68 (10,000)	This work

---

56

## 57 References

- 58 1. R. BoopathiRaja and M. Parthibavarman, *Electrochimica Acta*, 2020, **346**, 136270.  
59 2. F. Wang, X. Lv, L. Zhang, H. Zhang, Y. Zhu, Z. Hu, Y. Zhang, J. Ji and W. Jiang, *Journal of Power*  
60 *Sources*, 2018, **393**, 169-176.  
61 3. D. Kong, W. Ren, C. Cheng, Y. Wang, Z. Huang and H. Y. Yang, *ACS applied materials & interfaces*,  
62 2015, **7**, 21334-21346.  
63 4. T. H. Ko, D. Lei, S. Balasubramaniam, M.-K. Seo, Y.-S. Chung, H.-Y. Kim and B.-S. Kim,  
64 *Electrochimica Acta*, 2017, **247**, 524-534.  
65 5. L. He, Z. Guo, G. Wang and M. Li, *Journal of Energy Storage*, 2024, **79**, 110130.  
66 6. S. Sathishkumar, M. Karthik, R. Boopathiraja, M. Parthibavarman, S. Nirmaladevi and S.  
67 Sathishkumar, *J Mater Sci.: Mater Electron* 2022, **33**, 21600-21614.  
68 7. A. Sathiyar, E. Elaiyappillai, S.-F. Wang, S. Dhineshkumar and P. M. Johnson, *New Journal of*  
69 *Chemistry*, 2024, **48**, 3080-3088.  
70 8. J. Yu, D. Yao, Z. Wu, G. Li, J. Song, H. Shen, X. Yang, W. Lei, F. Wu and Q. Hao, *ACS Applied Energy*  
71 *Materials*, 2021, **4**, 3093-3100.  
72 9. X. Li, H. Xie, Y. Feng, Y. Qu, L. Zhai, H. Sun, X. Liu and C. Hou, *Journal of Applied Polymer Science*,  
73 2023, **140**, e54580.  
74 10. A. Kathalingam, S. Ramesh, H. M. Yadav, J.-H. Choi, H. S. Kim and H.-S. Kim, *Journal of Alloys and*  
75 *Compounds*, 2020, **830**, 154734.  
76 11. S. Verma, V. K. Pandey and B. Verma, *Synthetic Metals*, 2022, **286**, 117036.  
77 12. S. Verma, T. Das, V. K. Pandey and B. Verma, *Journal of Molecular Structure*, 2022, **1266**,  
78 133515.

- 79 13. Z. Chen, X. Zu, L. Chen, Y. Qi, W. Jian, Y. Wu, W. Zhang, X. Lin, G. Yi and Q. Liu, *ACS Applied*  
80 *Energy Materials*, 2022, **5**, 5937-5946.
- 81 14. H. M. Fahad, R. Ahmad, F. Shaheen, A. A. Ifseisi, M. H. Aziz and Q. Huang, *Electrochimica Acta*,  
82 2024, 143756.
- 83 15. S. K. Shinde, S. S. Karade, N. T. N. Truong, S. S. Veer, S. F. Shaikh, A. M. Al-Enizi, A. D. Jagadale, H.  
84 M. Yadav, M. S. Tamboli and C. Park, *Journal of Energy Storage*, 2024, **78**, 109960.

85